Hindawi
International Journal of Antennas and Propagation
Volume 2019, Article ID 7143274, 7 pages
https://doi.org/10.1155/2019/7143274

*Research Article*

# Dual-Mode Circular Polarization Selective Surface Cell for Single-Layer Dual-Band Circularly Polarized Reflectarray

**Zheng Liu, Xue Lei, Jun-Mo Wu, and Zhi-Jian Xu**

*School of Zhengzhou Information Science and Technology Institute, Zhengzhou 450002, China*

Correspondence should be addressed to Zheng Liu; lzfcsdcn@sina.com

Received 23 September 2018; Revised 12 January 2019; Accepted 3 February 2019; Published 26 June 2019

Academic Editor: N. Nasimuddin



A dual-mode circular polarization selective surface (CPSS) cell based on a modification of the Pierrot cell is presented for single-layer dual-band circularly polarized (CP) reflectarray antenna design. To achieve dual-mode CP discrimination performance, the improved three-dimensional geometry and the high-order resonances of the CPSS cell are utilized. The required phase shifts in both modes are obtained by varying the cell rotation angle. A single-layer dual-band reflectarray operating with orthogonal CPs has been fabricated and tested. Measured results show the peak gains of 25.2 dBi at 11.6 GHz with 31% 3 dB axial ratio (AR) bandwidth and 26.5 dBi at 14.6 GHz with 32% 3 dB AR bandwidth, respectively. The measured efficiency is 41.2% at 11.6 GHz and 55.5% at 14.6 GHz.

## 1. Introduction

Reflectarrays in multifunction integration such as multiband [1, 2] and multipolarization [3, 4] are in urgent needs for space communication with advantages in high capacity and low cost. Meanwhile, antenna operating in circular polarization (CP) is advantageous for extreme environments since it eliminates the polarization mismatch and restrains multipath interference. Typical multiband CP reflectarray consists of multiple resonators within one unit cell, such as dual split loop [2] and concentric split ring [5] elements. However, there are few researches on single-resonator multiresonance cell for CP reflectarray, which could simultaneously achieve simplification structure and multiband capability. The single-layer multiresonance broadband CP reflectarray has been proposed reaching more than 30% antenna bandwidth in [6]. The dual-CP reflectarray with independent control in the identical frequency was firstly researched in [3] based on the circular polarization selective surface (CPSS) cell.

CPSS reflects one sense of CP incident wave and is transparent to the other. The first CPSS structure was proposed theoretically by Pierrot in 1966 [7] as shown in Figure 1. In this Pierrot design, the cell is a $1\lambda$-long metallic wire folded into three segments, where the $3\lambda/8$-long transverse orthogonal segments are separated $\lambda/4$ in longitudinal direction by the vertical segment. As the left-handed CPSS (LHCPSS), LHCP incident wave is reflected and RHCP incident wave is transmitted, while the behaviors are inversed for the right-handed CPSS (RHCPSS).

A handful of researches on CPSS about improved performance [8] and structure [9] can be found in the last decade. Some different methods on CPSS design have been introduced in [7, 10]. CPSS filtering orthogonal CP waves could be used in polarization converter and other CP managements in single aperture [11]. Dual-CP reflectarray using the reconfigurable CPSS cell was studied by Mener et al. in [3, 12], which has been the sole form for CPSS's application to multifunction reflectarray design so far. Otherwise, the multimode CPSS with more stringent requirements has not been used, since that no simple electromagnetic structure achieving multimode CP discriminations has been known.

In this paper, a compact dual-mode CPSS cell is proposed, which could be used in single-layer dual-band CP reflectarray design. The RHCPSS is displayed in one mode

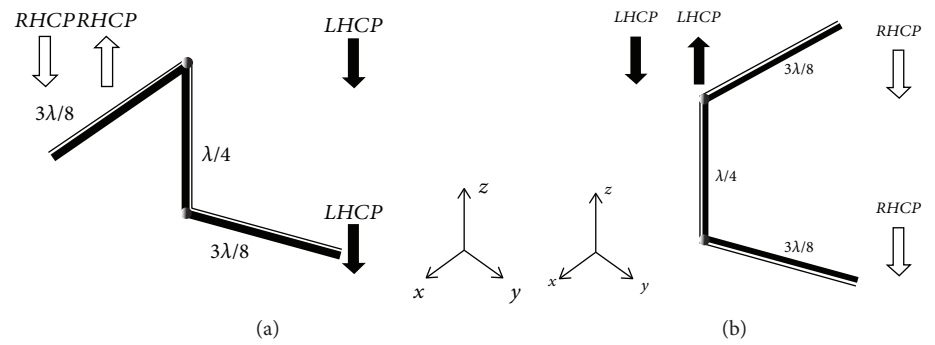


Figure 1: Pierrot cell configuration. (a) RHCPSS. (b) LHCPSS.

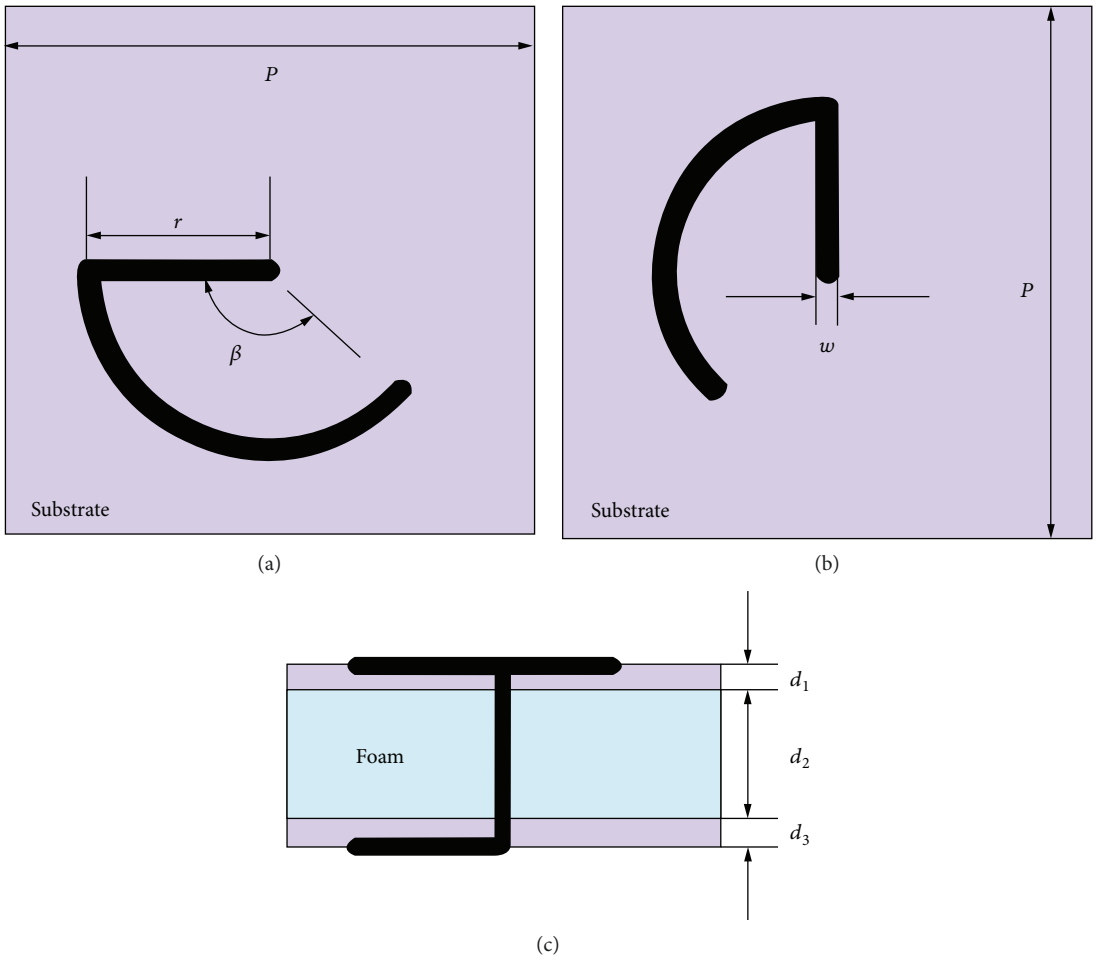


Figure 2: Geometry of the proposed dual-mode CPSS cell: (a) top view, (b) bottom view, and (c) side view.

while the LHCPSS is displayed in the other. A dual-band reflectarray in orthogonal CP waves based on the proposed cell is presented, together with the performance assessments in simulations and measurements.

## 2. Dual-Mode CPSS Cell Design for CP Reflectarray

*2.1. Cell Operation Principle.* As the Pierrot cell, the induced currents on both transverse orthogonal arms added in-phase or out-of-phase determine the CP sensitivity, and the $\lambda/4$ vertical distance ensures CP selection ability. In CP reflectarray, variable rotation technique (VRT) is used for phase steering. Thus, the rotatable element structure is required in each lattice. The periodicity should be reduced to $0.5\lambda$ to avoid grating lobe and get wider bandwidth. Furthermore, the whole length of the wire resonator should be equal to an integral multiple of the $0.5\lambda$ approximately, which is the prerequisite for geometrical resonance.

Thus, the bent horizontal metallic arms are adopted instead of the straight arms for dual-mode CPSS-based CP reflectarray cell design. The lengths of the whole metallic wire

and the each segment will not follow the original electrical size limitation. The proposed cell is schematically illustrated in Figure 2. Considering about the geometrical resonance and the CP selection performance, the primary parameters stem from

$$\begin{cases} f_n \approx \dfrac{(n+1)c}{2\left(2d_1\sqrt{\varepsilon_{\text{eff}}} + d_2 + 2r + 2r\beta\right)}, \quad n = 0, 1, 2, 3, \ldots, \\ \dfrac{c}{4f_n} \approx 2d_1\sqrt{\varepsilon_{\text{eff}}} + d_2 \end{cases} \tag{1}$$

where $n$ is the number of the current nulls along the entire wire in mode $n$, $\varepsilon_{\text{eff}}$ is effective dielectric constant of the substrate layer, $c$ is the speed of light, and the other parameters refer to Figure 2. Mode 2 and mode 3 are taken into account to decrease the length difference between the adjacent modes and reduce cross-polarization components. The Ku band is interested for satellite communication application.

Element simulations were performed using the CST Microwave Studio in the periodic structure optimization process with two Floquet ports ($Z_{\max}$ port and $Z_{\min}$ port). All of the parameters affect the selection characteristics, and the cell design parameters ($\beta$, $r$) influence mode 3 resonance frequency significantly. Tradeoffs have to be made in parameters optimization by genetic algorithm as shown in Figure 3. The foremost optimum targets are good reflection and transmission coefficients in both modes, and then the cross-polarizations should be considered. The final dimensions are as follows: $p = 12.5$ mm, $d_1 = 0.5$ mm, $d_2 = 4$ mm, $r = 5$ mm, $w = 0.3$ mm, and $\beta = 0.76\pi$rad.

*2.2. Simulation Results.* The comparison of CP selection characteristics between the dual-mode CPSS cell and the classical CPSS cell (see Figure 1(a)) is shown in Figures 4 and 5. The classical CPSS cell operates at 12 GHz with single CP selection mode, while the proposed CPSS cell possesses two orthogonal CP selection modes. The resonance current distributions of the proposed cell in each mode are depicted in Figure 6. Mode 2 resonates under RHCP incidence with two current nulls, operating over the frequency range 11.8–12.7 GHz ($S_{11}^{\text{RR}} > -1$ dB, $S_{21}^{\text{LL}} > -1.2$ dB), and the axial ratios (ARs) are less than 2.1 dB in both reflection and transmission cases; mode 3 resonates under LHCP incidence with three current nulls, operating over the frequency range 14.9–15.8 GHz ($S_{11}^{\text{LL}} > -1$ dB, $S_{21}^{\text{RR}} > -1.4$ dB), and ARs are less than 4.9 dB in both cases. Thus, RHCPSS is displayed in mode 2, and LHCPSS is displayed in mode 3.

Compared with the classical CPSS, the proposed CPSS cell behaves obvious dual-mode CP selection characteristic. But it is regretful that the transmission losses in two modes are impacted slightly by nonorthogonal transverse current distributions from the bent arms, which increase the reflection components in transmission cases. Increased cross-polarized terms in mode 3 caused by the more complex current distribution deteriorate ARs inevitably. Even so, the modified CPSS structure and high-order resonances are crucial for dual-mode CPSS performance.

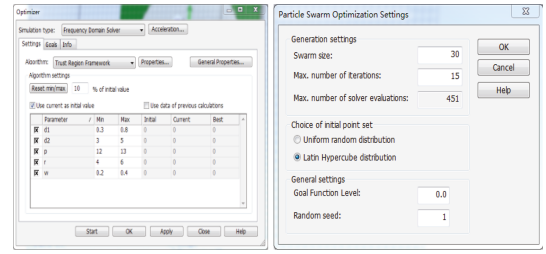


Figure 3: Optimization of the cell in the CST Microwave Studio.

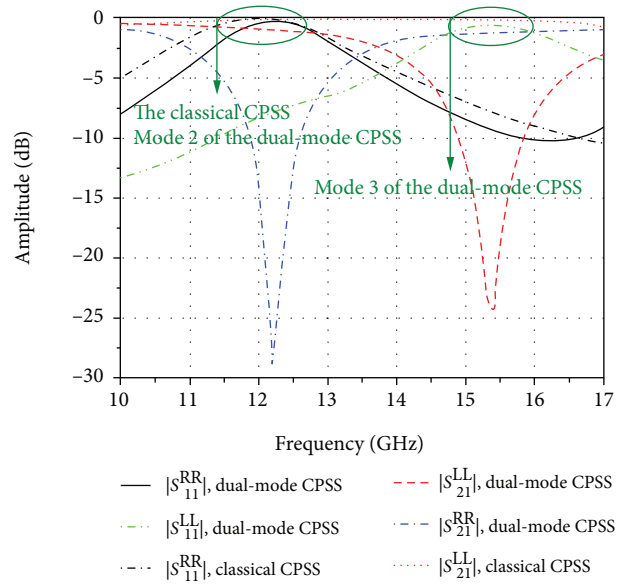


Figure 4: Comparison of the CP discrimination capabilities between the dual-mode CPSS and the classical CPSS.

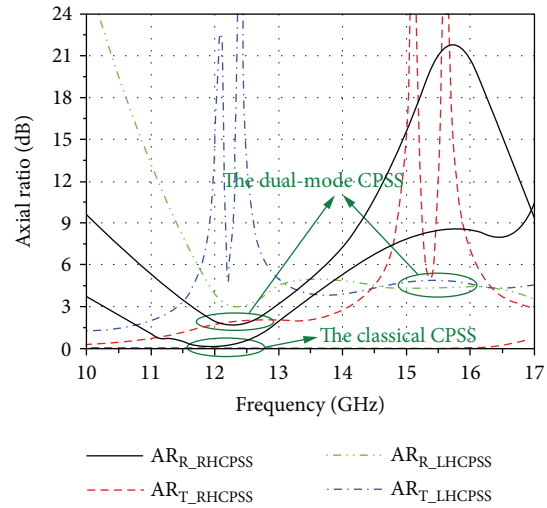


Figure 5: Comparison of the ARs between the dual-mode CPSS and the classical CPSS in reflection and transmission cases.

For CP reflectarray application, the good linearity phase curves in both modes are demonstrated in Figure 7. It should be mentioned that the phase compensations have been reversed with the rotated element under orthogonal

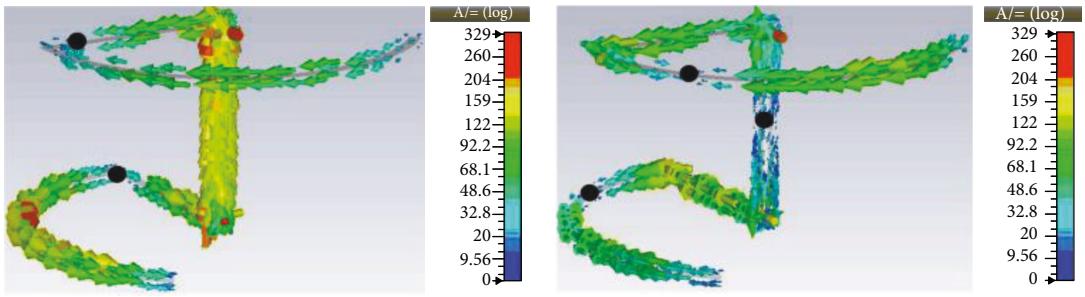


(a) (b)

Figure 6: Current distributions of two modes: (a) mode 2 resonance at 12.2 GHz under LHCP with two nulls and (b) mode 3 resonance at 15.4 GHz under RHCP with three nulls.

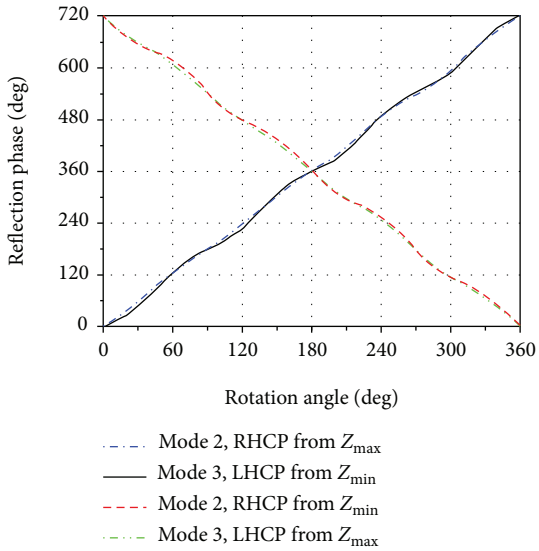


Figure 7: Phase curves of the dual-mode CPSS cell for LHCP and RHCP plane-wave incidences from both sides of the cell at mode 2 and mode 3. Phase response for different angles of incidence for TE mode.

CP incident waves from the same port. Thus, the RHCP and LHCP horns should illuminate from the opposite sides of the reflectarray to obtain accurate phase correction on each aperture.

## 3. Single-Layer Dual-Band CP Reflectarray

The CPSS cell has been applied to dual-CP reflectarray [3], but not been used in other multifunction reflectarray designs. Using the PCB fabrication technique, the single-layer single-resonator dual-band reflectarray based on the dual-mode CPSS cell is fabricated and tested. Photographs of the manufactured reflectarray are shown in Figure 8. The size of the reflectarray is $200 \times 200$ mm$^2$.

The bent transverse metallic arms are printed on two thin F4B ($\varepsilon_r = 2.2$, $\tan\delta = 0.0009$) substrates, respectively. A piece of foam layer is placed between them to minimize reflection. The copper wires with the diameter equal to the width of the transverse arms are used as the vertical metal conductors in each unit. The both ends of the copper wires are connected to the transverse metallic arms and fixed by soldering. The reflectarray was illuminated by the RHCP horn from one side and then illuminated by the identical LHCP horn from the other side. The F/D ratios are 0.6 and the distances between the horn phase centers and the apertures are both 120 mm.

Radiation patterns of the focused beams with inverse orientations at 11.6 GHz and 14.6 GHz are plotted in Figure 9. At 11.6 GHz, the peak sidelobe level is -18 dB, and the maximum cross-polarization level is -23.4 dB. At 14.6 GHz, the peak sidelobe and cross-polarization levels are -18.6 dB and -28.8 dB, respectively. Figure 10 shows the measured gains and axial ratios versus frequency throughout both bands. The peak gains of 25.2 dBi and 26.5 dBi are obtained, with the efficiencies of 41.2% and 55.5%, respectively. Furthermore, the 1 dB gain bandwidths are 7.8% for RHCP (11.1 GHz-12 GHz) and 8.2% for LHCP (13.9 GHz-15.1 GHz). The ARs are kept below 1.6 dB in both bands. The drawback of the cell's AR in reflection case at mode 3 is remedied by mutual coupling in practical array environment. As a dual-mode CPSS array, the insertion losses are considered in Figure 11, which are corresponding to the reflection characteristics depicted in Figure 10.

Compared with the classical CPSS [13], the CPSS-based reflectarray [3], and the dual-band reflectarray in orthogonal CPs [14], as summarized in Table 1, a CPSS-based dual-band CP reflectarray has been achieved. The cell can be used in other types of multifunction CP reflectarrays for space communication as well.

## 4. Conclusion

The dual-mode CPSS cell and the dual-band CP reflectarray based on it are studied in this paper. The proposed cell displays RHCPSS in one mode and displays LHCPSS in the other. The dual-band CP reflectarray consists of the cell is designed with performance assessments in simulations and measurements. This paper provides more functions and increases practicality value in developing CPSS. The dual-band dual-CP reflectarray and other CP devices based on the novel CPSS cell will be investigated deeply in future for space communication.

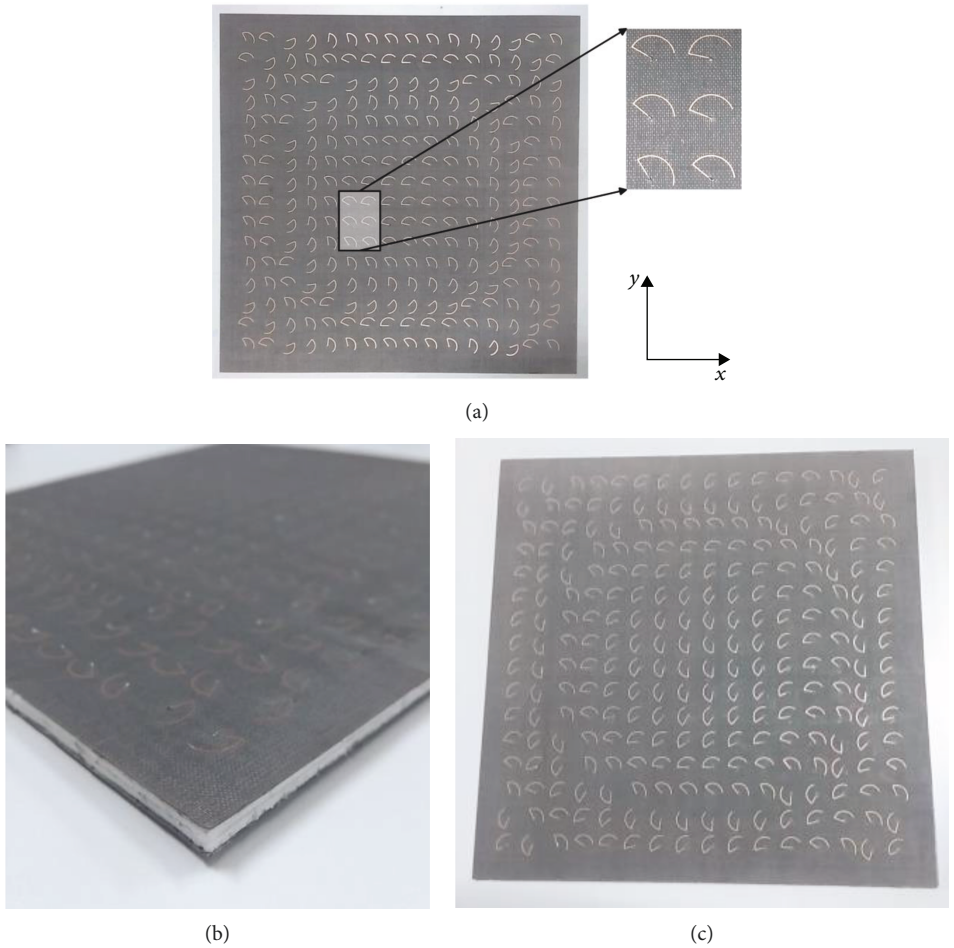


Figure 8: Photographs of the dual-band CP reflectarray: (a) top view, (b) side view, and (c) bottom view.

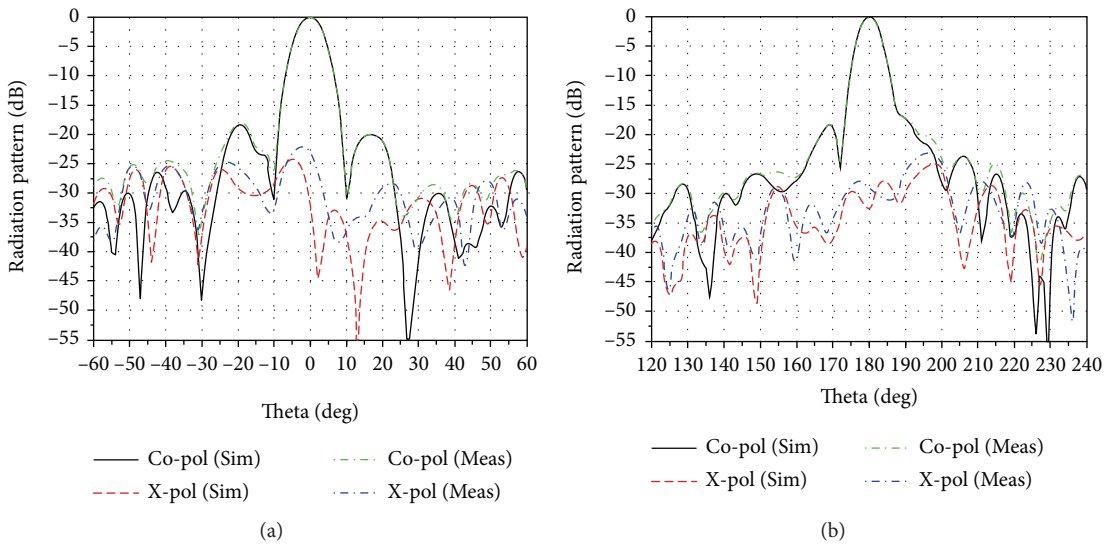


Figure 9: Measured and simulated radiation patterns of the fabricated reflectarray at (a) 11.6 GHz and (b) 14.6 GHz. The LHCP and RHCP feeds are placed on each side of the reflectarray, respectively.

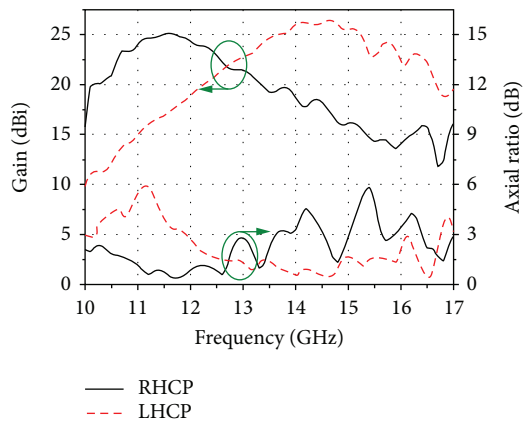


Figure 10: Measured gains and axial ratios of the reflectarray versus frequency under RHCP and LHCP illuminations.

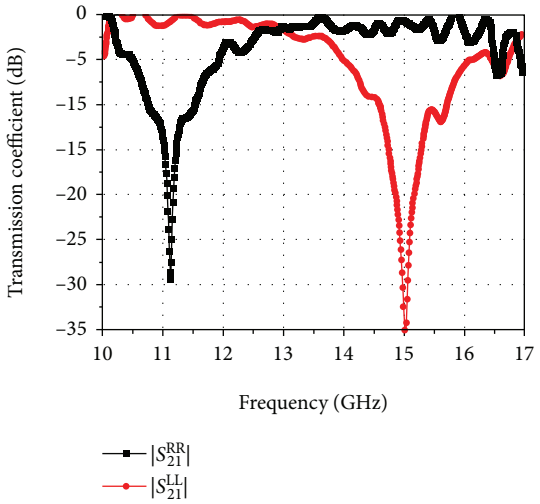


Figure 11: Measured transmission coefficients of the reflectarray versus frequency under RHCP and LHCP illuminations.

Table 1: Comparison with existing relevant works.

| | [13] | [3] | [14] | This work |
|---|---|---|---|---|
| Available in RA? | N* | Y* | Y | Y |
| Available in CPSS? | Y | Y | N | Y |
| Available in dual-band? | N | N | Y | Y |
| Frequency (GHz) | 9.8 | 8.37 | 20.6/30.4 | 11.6/14.6 |
| Gain (dBi) | — | About 21 | 36.1/40.5 | 25.2/26.5 |
| Efficiency (%) | — | 25 | 40/50 | 41.2/55.5 |
| 1 dB gain BW (%) | — | 9.4 (1.5 dB gain) | — | 7.8/8.2 |
| AR BW (%) | — | 9.4 (3.5 dB AR) | — | 31/32 (3 dB AR) |
| Insertion loss (dB) | 0.2 | — | — | 1.2/-2.2 |

*Y means yes and N means no.

## Data Availability

The data used to support the findings of this study are available from the corresponding author upon request. Requests for access to these data should be made by Zheng Liu at lzfcsdcn@sina.com.

## Conflicts of Interest

The authors declare that there is no conflict of interest regarding the publication of this paper.

## References

[1] H. Hasani, M. Tamagnone, S. Capdevila et al., "Tri-band, polarization-independent reflectarray at terahertz frequencies: design, fabrication, and measurement," *IEEE Transactions on Terahertz Science and Technology*, vol. 6, no. 2, pp. 268–277, 2016.

[2] T. Smith, U. Gothelf, O. S. Kim, and O. Breinbjerg, "Design, manufacturing, and testing of a 20/30-GHz dual-band circularly polarized reflectarray antenna," *IEEE Antennas and Wireless Propagation Letters*, vol. 12, pp. 1480–1483, 2013.

[3] S. Mener, R. Gillard, R. Sauleau, A. Bellion, and P. Potier, "Dual circularly polarized reflectarray with independent control of polarizations," *IEEE Transactions on Antennas and Propagation*, vol. 63, no. 4, pp. 1877–1881, 2015.

[4] R. Florencio, J. A. Encinar, R. R. Boix, V. Losada, and G. Toso, "Reflectarray antennas for dual polarization and broadband telecom satellite applications," *IEEE Transactions on Antennas and Propagation*, vol. 63, no. 4, pp. 1234–1246, 2015.

[5] C. Guclu, J. Perruisseau-Carrier, and O. Civi, "Proof of concept of a dual-band circularly-polarized RF MEMS beam-switching reflectarray," *IEEE Transactions on Antennas and Propagation*, vol. 60, no. 11, pp. 5451–5455, 2012.

[6] M.-Y. Zhao, G. Q. Zhang, X. Lei, J. M. Wu, and J. Y. Shang, "Design of new single-layer multiple-resonance broadband circularly polarized reflectarrays," *IEEE Antennas and Wireless Propagation Letters*, vol. 12, pp. 356–359, 2013.

[7] J. E. Roy and L. Shafai, "Reciprocal circular-polarization-selective surface," *IEEE Antennas and Propagation Magazine*, vol. 38, no. 6, pp. 18–33, 1996.

[8] S. M. A. Momeni Hasan Abadi and N. Behdad, "A broadband, circular-polarization selective surface," *Journal of Applied Physics*, vol. 119, no. 24, article 244901, 2016.

[9] C. Cappellin, D. Sjoberg, A. Ericsson et al., "Design and analysis of a reflector antenna system based on doubly curved circular polarization selective surfaces," in *2016 10th European Conference on Antennas and Propagation (EuCAP)*, pp. 1–5, Davos, Switzerland, April 2016.

[10] J. Wang, W. Wu, and Z. Shen, "Circular polarization selective structure based on planar helix," in *2017 IEEE International Symposium on Antennas and Propagation & USNC/URSI National Radio Science Meeting*, pp. 1861-1862, San Diego, CA, USA, July 2017.

[11] V. F. Fusco and B. Nair, "Circular polarisation selective surface characterisation and advanced applications," *IEE Proceedings - Microwaves, Antennas and Propagation*, vol. 153, no. 3, pp. 247–252, 2006.

[12] S. Mener, R. Gillard, R. Sauleau, C. Cheymol, and P. Potier, "Unit cell for reflectarrays operating with independent dual circular polarizations," *IEEE Antennas and Wireless Propagation Letters*, vol. 13, pp. 1176–1179, 2014.

[13] J. Sanz-Fernandez, E. Saenz, and P. de Maagt, "A circular polarization selective surface for space applications," *IEEE Transactions on Antennas and Propagation*, vol. 63, no. 6, pp. 2460–2470, 2015.

[14] M. R. Chaharmir and J. Shaker, "Design of a multilayer X-/Ka-band frequency-selective surface-backed reflectarray for satellite applications," *IEEE Transactions on Antennas and Propagation*, vol. 63, no. 4, pp. 1255–1262, 2015.